NOCMAT 2026, v.1, e003

abmtenc

NOCMAT

https://periodicos.uefs.br/index.php/nocmat

ISSN
XXXX-XXXX

Influence of Mineral Fillers and Curing Conditions on the Hydration, Microstructure, and Mechanical Performance of MgO-Based Cements

Influência de fillers minerais e das condições de cura na hidratação, microestrutura e desempenho mecânico de cimentos à base de MgO

MOLANO, Juan Camilo Adrada[1*]; LIRA, Douglas Sadalla[1]; AZEVEDO, Adriano Galvão[1]; CORDOBA, Katheryn Pallares; SAVASTANO JR, Holmer[1]

1 Departamento de Engenharia de Biossistemas, Centro de Pesquisa em Materiais para Biossistemas (BioSMat), Universidade de São Paulo (USP), São Paulo, Pirassununga, Brasil

* Correspondent author: camiloadrada@gmail.com

Received: March 13, 2026
Accepted: August 7, 2026
Published: September, 1,2026

Citation: J. C. A. Molano, D. S. Lira, A. G. Azevedo, K. P. Cordoba, and H. Savastano Jr., "Influence of mineral fillers and curing conditions on the hydration, microstructure, and mechanical performance of MgO-based cements," *NOCMAT*, vol. 1, e003, 2026. DOI:

Abstract
Magnesium oxysulfate (MOS) cement, also known as basic magnesium sulfate cement (BMSC), is a low-alkalinity binder with potential for sustainable construction due to its lower calcination requirements and compatibility with alternative magnesium oxide sources. This study investigated the effects of partially replacing MgO with limestone filler and the addition of citric acid (AC) on hydration phase formation, physical properties, and mechanical performance of MOS cement. The influence of curing conditions was evaluated using mixtures containing calcitic limestone to isolate the curing effect, while filler comparison was conducted under ambient curing (23 ± 2 °C and 60% relative humidity). Results showed that mixtures without AC mainly formed the 318 phase, $Mg(OH)_2$, and residual periclase, together with carbonate phases such as dolomite, magnesite, calcite, and aragonite. The addition of AC promoted the formation of the 517 phase, leading to an increase of up to 78% in compressive strength compared to the reference MOS cement. The highest strengths were obtained under curing at 80% relative humidity, whereas thermal curing (60 °C and 90% RH) resulted in lower mechanical performance due to increased brucite formation.
Keywords: Magnesium cement, oxysulfate, filler, limestone, mechanical strength.

Resumo
O cimento oxissulfato de magnésio (MOS), também conhecido como cimento básico de sulfato de magnésio (BMSC), é um ligante de baixa alcalinidade com potencial para aplicações em construção sustentável, devido aos menores requisitos de calcinação e à compatibilidade com fontes alternativas de óxido de magnésio. Este estudo investigou os efeitos da substituição parcial do MgO por *filler* calcário e da adição de ácido cítrico (CA) na formação das fases de hidratação, propriedades físicas e desempenho mecânico do cimento MOS. A influência das condições de cura foi avaliada utilizando misturas com calcário calcítico, permitindo isolar o efeito dos regimes de cura, enquanto a comparação entre *fillers* foi realizada sob cura em temperatura ambiente (23 ± 2 °C e 60% de umidade relativa). Os resultados indicaram que misturas sem CA formaram predominantemente a fase 318, $Mg(OH)_2$ e periclásio, além de fases carbonatadas como dolomita, magnesita, calcita e aragonita. A adição de CA promoveu a formação da fase 517, resultando em aumento de até 78% na resistência à compressão em relação ao MOS de referência. As maiores resistências foram observadas sob cura a 80% de umidade relativa, enquanto a cura térmica (60 °C e 90% UR) resultou em menor desempenho mecânico devido à maior formação de brucita.
Palavras-chave: Cimento magnesiano, oxissulfato, *filler*, calcário, resistência mecânica.

1 INTRODUCTION

Magnesium oxysulfate (MOS) cement was developed in 1867 and constitutes a type of MgO-based cement, analogous to Sorel cement, in which magnesium oxide is combined with a magnesium chloride ($MgCl_2$) solution to form a non-hydraulic binder. Similarly, magnesium oxysulfate cement can be obtained by the reaction between magnesium oxide (MgO) and an aqueous magnesium sulfate ($MgSO_4$) solution [1, 2]. This type of non-hydraulic binder presents advantages such as low density, low energy consumption, and good thermal insulation properties [3, 4]. In addition, MOS exhibits high resistance to acids, bases, and saline environments, as well as excellent adhesion performance [2, 5-7]. For these reasons, its application potential has been explored in different areas, including MOS-based concretes, porous thermal insulation materials, fire-resistant boards, composite panels, decorative panels,

prefabricated elements, and the immobilization of heavy metals and solid waste, demonstrating its broad applicability in the construction industry [3-6, 8, 9].

Another relevant aspect is that MgO, under suitable curing conditions, can undergo carbonation reactions due to the absorption of carbon dioxide (CO_2), resulting in both mechanical strength gain and reduced CO_2 emissions [10, 11]. Analogously to the production of ordinary Portland cement (OPC) from limestone, MgO can be obtained by calcination of magnesite ($MgCO_3$), although at lower temperatures (approximately 1450 °C for OPC and 750 °C for MgO), which implies lower energy consumption in the process [9, 12]. In addition to magnesite, MgO can also be produced from seawater, brines, or waste generated from desalination processes [13, 14]. Thus, due to the combination of lower energy consumption, CO_2 capture potential, and wide availability of magnesium-bearing minerals, MgO-based cements have been receiving increasing attention. According to the Mineral Commodity Summaries 2022 report, approximately 30,000 tons of magnesium-containing compounds were extracted from mines in 2021, with approximately 2,000 tons produced in Brazil [15]. However, studies on MgO-based construction materials are still limited, reinforcing the need for further investigation to optimize their performance and applications.

The final properties of MOS cement essentially depend on the hydration products formed after the pastes harden [5]. According to the ternary MgO–$MgSO_4$–H_2O system, four oxysulfate phases can form between 30 °C and 120 °C: (I) $3Mg(OH)_2 \cdot MgSO_4 \cdot 8H_2O$ (phase 318), (II) $5Mg(OH)_2 \cdot MgSO_4 \cdot 3H_2O$ (phase 513), (III) $Mg(OH)_2 \cdot MgSO_4 \cdot 5H_2O$ (phase 115), and (IV) $Mg(OH)_2 \cdot 2MgSO_4 \cdot 3H_2O$ (phase 123) [16-18]. Among them, phase 318 is the most stable at temperatures close to 23 °C, exhibiting better physical-mechanical performance and greater chemical stability, which are fundamental properties for the durability and strength of the cement, particularly for MOS produced without chemical additives [17].

Low mechanical strength and, especially, limited stability in humid environments represent some of the main challenges for the industrial applications of MOS cements. This occurs due to delayed hydration of MgO under high-humidity conditions, which can generate microcracks in the cement and consequently cause a decrease in mechanical performance [19]. In 2005, Deng Dehua [20] reported a new hydration product produced with chemical additives that has the ability to considerably increase the mechanical strength and stability of the cement under thermal and high-humidity conditions. More recently, Runcevski *et al*. [21], successfully analyzed the chemical composition and crystal structure of the new hydration product using modern techniques, discovering that a new MOS phase crystallizes with a stoichiometry of $5Mg(OH)_2 \cdot MgSO_4 \cdot 7H_2O$ (phase 517). This new type of MgO-$MgSO_4$-H_2O-based cementitious material is referred to as basic magnesium sulfate cement (BMSC) [22].

The formation of hydration phases depends mainly on the mixture composition, with the molar concentrations of MgO, $MgSO_4$, and H_2O being the determining parameters [23, 24]. Tang *et al.* [24], evaluated the influence of the $MgSO_4/H_2O$ ratio on the evolution of paste porosity using non-contact impedance measurements (NCIMs). It was found that a decrease in this ratio reduced the formation kinetics of the hydration products, identified by mass loss between 80 and 250 °C, associated with the dehydration of the phases responsible for the material's strength. Conversely, an increase in the $MgO/MgSO_4$ ratio intensified the formation of phases 517 and 318, resulting in greater mass losses and strength gain. In the same study, it was also observed that excess water in BMSC synthesis reduced compressive strength at all curing ages, in addition to significantly altering the porous microstructure (total porosity, incremental volume, tortuosity, mean diameter, and maximum pore diameter) [23].

The incorporation of fillers into cementitious materials, as partial binder replacements, has been an established practice since the 1980s [25]. Fillers are low-reactivity materials, mainly employed to promote physical effects, such as void filling, improvement of particle size distribution, and microstructure densification [25]. In parallel, reactive supplementary cementitious materials, such as fly ash, blast furnace slag, silica fume, and metakaolin, have also been widely used, contributing chemically to the performance of cementitious composites [26]. In the case of limestone fillers, this replacement offers environmental advantages, since their production does not require calcination processes [27].

While the production of MgO by calcination of magnesite releases approximately 3.1–4.5 kg CO_2eq/kg of MgO, filler production emits only 26–75 g CO_2/kg [27, 28]. In addition, limestone filler can act in the absorption of the heat released during the exothermic formation of cement, reducing thermal shocks [29], and contribute to microstructure densification through the filler effect [30]. It has also been reported that its addition favors CO_2 diffusion in cement pastes [31]. Li *et al.* [32] demonstrated that partial replacement of MgO with lime (CaO) in reactive magnesium cements (RMC) increased CO_2 absorption capacity, both under ambient conditions and accelerated carbonation. Despite the extensive investigation of the use of limestone fillers in Portland cements, studies on their application in MOS cements remain scarce. Gomes and de Oliveira [33], for example, evaluated the replacement of MgO with carbonates, observing improvements in hydration control.

In the present study, limestone fillers from different sources were used, including calcitic limestone, dolomitic limestone, and oyster shell powder. The choice of these materials was motivated by their availability, low cost, and potential for sustainable application in MgO-based cementitious systems. Dolomitic limestone (CD), for example, is a low-cost and non-toxic mineral, rarely used in Portland cements due to expansion problems related to its MgO content, but widely used as a pH corrector in agricultural applications [34, 35].

With the objective of evaluating the effect of limestone incorporation into basic magnesium sulfate cements (BMSC), this study investigates the MgO–$MgSO_4$–H_2O system modified with chemical additives and mineral limestone fillers. The formulations were prepared with a molar ratio of n(MgO):n($MgSO_4$):n(H_2O) of 10:1:20, with the addition of citric acid (AC) at 0.5% by mass of MgO to promote the formation of phase 517. Limestone fillers were incorporated as partial replacements for MgO in order to evaluate their effect on the formation of hydration phases, microstructure, and mechanical performance of BMSC pastes. Thus, the aim is to understand the mechanisms associated with the incorporation of these materials and contribute to the development of formulations with optimized performance and lower environmental impact.

2 MATERIALS AND METHODS

2.1 MATERIALS

Magnesium oxide (MgO), used as the main precursor in the basic magnesium sulfate cement (BMSC) matrix, was light-burned magnesia (LBM), produced by the controlled calcination of magnesite at approximately 1050 °C and supplied by RHI Magnesita (Contagem, MG, Brazil). The material presented a specific surface area of 26.71 m²/g and a density of 3.45 g/cm³. The chemical composition and particle size distribution (D_{50} = 22.20 μm) presented in Figure 1, Table 1, and Table 2 were determined by X-ray fluorescence (XRF, Malvern Panalytical Zetium) and laser scattering (Horiba LA-950, Kyoto, Japan), respectively.

The WB/T1019 hydration test [36], was used to determine the active MgO (α-MgO) content of the LBM. According to Dong *et al.* [37], only active magnesium oxide can react with water to form $Mg(OH)_2$. Based on this perspective, the α-MgO content in magnesium oxide can be determined using Eq. 1. The active magnesia content of the LBM in this study was approximately 64%.

$$\alpha - MgO = \frac{40(m_2 - m_1)}{18m_1} \quad (1)$$

where m_1 is the mass (g) of the LBM before reacting with water, and m_2 is the mass (g) after reacting with water for three hours at 105 °C and drying at 105 °C for 24 h to remove all water that had not been chemically combined.

Table 1: Characteristic diameters of the particle size distribution of light-burned MgO (LBM)

D_{10} (µm)	D_{50} (µm)	D_{90} (µm)
2.7	22.2	75.6

Figure 1: Discrete and cumulative particle size distribution of LBM

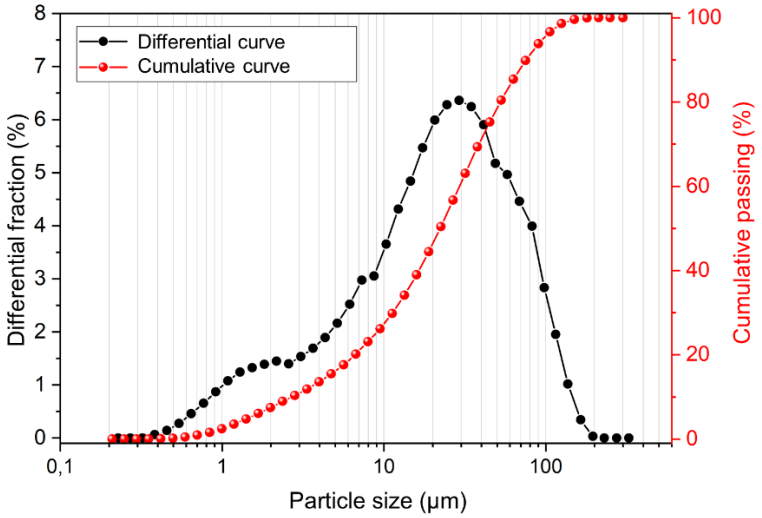

Table 2: Chemical composition of LBM

Material	(%) Mass*								
	MgO	Al_2O_3	SiO_2	SO_3	Cl	CaO	MnO	Fe_2O_3	LOI
LBM	94.1	0.09	0.28	0.26	0.06	1.47	0.18	0.91	2.62

*0,01 – XRF quantification limit

2.1.1 Dolomitic limestone

Dolomitic limestone (CD) and calcitic limestone (CC), used as mineral fillers in the BMSC compositions, were supplied by Infibra S.A. (Leme, SP, Brazil). The materials presented bulk densities of 2.79 g/cm³ and 2.77 g/cm³ and mean particle sizes (D_{50}) of 22.20 µm and 17.4 µm, respectively (Table 3). The chemical composition of the limestones and the loss on ignition (LOI) values are presented in Table 4, and the particle size distribution is shown in Figure 2.

The incorporation of limestone into the cementitious matrix contributes to the absorption of the heat released during the exothermic hydration reaction, reducing thermal shocks [29]. In addition, it can promote microstructure densification through the filler effect [30] and favor carbon dioxide diffusion in pastes [31]. Both CD and calcitic limestone (CC) were evaluated to compare the effect of the MgO content in the fillers on the mechanical properties of BMSC.

Table 3: Characteristic diameters of the particle size distributions of the limestones.

Material	D_{10} (µm)	D_{50} (µm)	D_{90} (µm)
Dolomitic limestone	3.4	23.1	71.6
Calcitic limestone	1.8	17.4	116.2

Table 4: Chemical composition of CD and CC

Material	(%) Mass*								
	MgO	Al_2O_3	SiO_2	SO_3	K_2O	CaO	MnO	Fe_2O_3	LOI
CD	7.60	1.03	3.99	0.13	0.22	43.9	0.09	0.42	42.4
CC	1.34	0.70	2.91	0.08	0.18	51.5	0.05	0.38	42.9

*0,01 - XRF quantification limit

Figure 2: Discrete and cumulative particle size distribution of CD and CC.

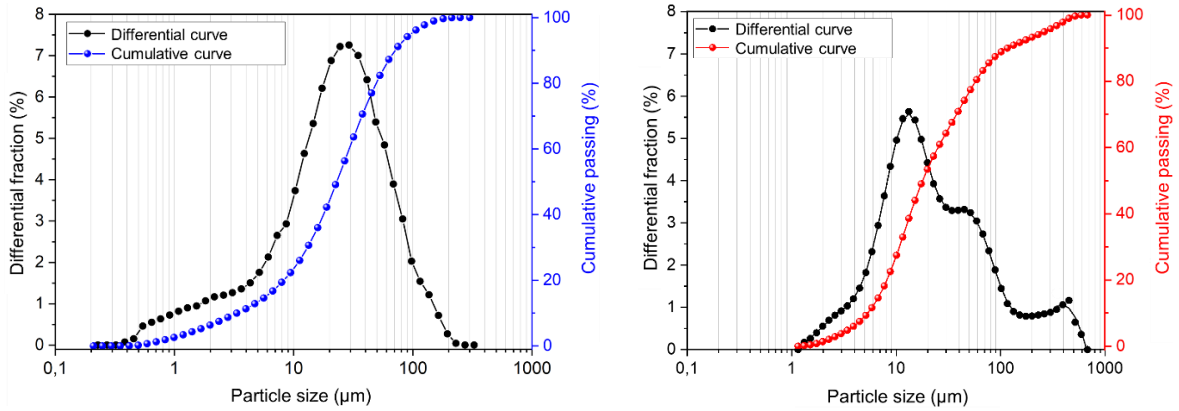

(A) Dolomitic limestone (CD) (B) Calcitic limestone (CC)

2.1.2 Oyster shell powder

As an alternative source of limestone, oyster shell powder (OSP) was commercially acquired from CYSY Mineração (Jaguaruna, SC, Brazil). The original material presented particles between 1.0 mm and 3.2 mm and was subjected to grinding in a ball mill with a metallic grinding medium for 4 h, followed by sieving through a #200 mesh (75 µm), obtaining the fraction with a suitable particle size for use as a mineral filler. The OSP presented a bulk density of 2.84 g/cm³ and a mean particle size (D_{50}) of 19.03 µm (Table 6). The chemical composition and loss on ignition (LOI) are presented in Table 5, and the particle size distribution is shown in Figure 3.

Table 3: Chemical composition of oyster shell powder (OSP)

Material	**(%) Mass***								
	MgO	Al_2O_3	SiO_2	SO_3	K_2O	CaO	MnO	Fe_2O_3	LOI
OSP	0.51	0.49	0.88	2.49	0.14	93.54	0.01	0.01	48.8

*0,01 - XRF quantification limit

Table 4: Characteristic diameters of the particle size distribution of OSP.

D_{10} (µm)	**D_{50} (µm)**	**D_{90} (µm)**
1.1	19.03	89.4

Figure 3: Discrete and cumulative particle size distribution of OSP

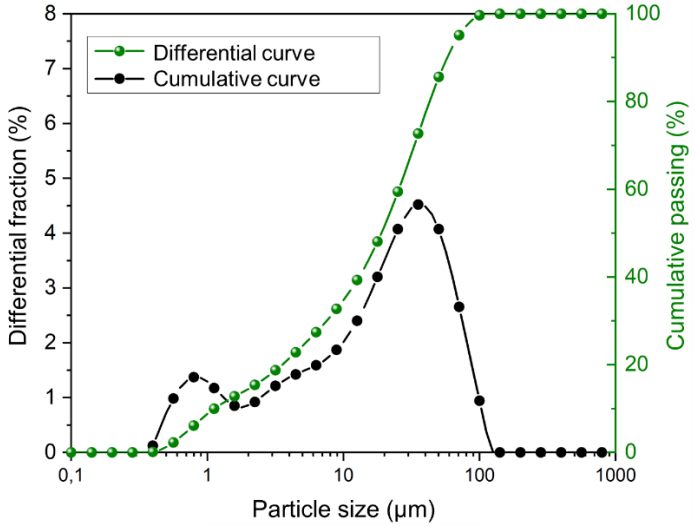

2.1.3 Magnesium sulfate heptahydrate

Magnesium sulfate heptahydrate ($MgSO_4 \cdot 7H_2O$), used to prepare the $MgSO_4$ solution, was purchased from LabSynth (Diadema, SP, Brazil), with a purity of 99.83%. Analytical-grade citric acid (AC) was used as a chemical additive to promote the formation of the 5-1-7 hydration phase, as it is the weak acid most commonly used as a modifier in BMSC systems [38-40].

2.2 SAMPLE PREPARATION

Basic magnesium sulfate cement (BMSC) pastes were prepared by mixing magnesium oxide (MgO), limestone filler, magnesium sulfate, and citric acid. $MgSO_4 \cdot 7H_2O$ was previously dissolved in water at approximately 60 °C, resulting in a solution with a concentration of 25% (w/v) $MgSO_4$. This temperature was selected to increase the solubility of the salt and ensure complete dissolution and homogeneity of the solution, since lower temperatures resulted in incomplete dissolution. The molar ratio adopted in the mixtures was $n(MgO):n(MgSO_4):n(H_2O)$ = 10:1:20, according to previous results obtained by the BioSMat group and recent studies on BMSC cements [19, 41, 42].

Initially, the MgO powder was homogenized with the respective filler (dolomitic limestone or oyster shell powder) for 1 min in a mixer at 500 rpm. Subsequently, the solid mixture was gradually added to the $MgSO_4$ solution under constant stirring at 1200 rpm and maintained under mixing for an additional 4 min, resulting in homogeneous pastes with uniform consistency. Citric acid (AC) was added as a chemical modifier in some compositions (BMSC), at a proportion of 0.5% by mass relative to MgO; its dissolution was carried out in the $MgSO_4$ solution. The proportions of each mixture and the corresponding coding are presented in Table 6, detailing the formulations containing dolomitic limestone (CD) and oyster shell powder (OSP), with and without the addition of citric acid.

Table 6: Composition of BMSC + limestone pastes.

Cod.	Molar ratio $MgO:MgSO_4:H_2O$	Dolomitic-calcitic limestone (% by mass of MgO)	Oyster shell powder (% by mass of MgO)	Citric acid (% by mass of MgO)
MOS Ref	10:1:20	-	-	-
MOS CD	10:1:20	20	-	-
BMSC CD+AC	10:1:20	20	-	0.5
MOS OSP	10:1:20	-	20	-
BMSC OSP+AC	10:1:20	-	20	0.5
BMSC+CC	10:1:20	20	-	0.5

The pastes were molded in acrylic cubic molds with nominal dimensions of 40 × 40 × 40 mm³ (Figure 4) for mechanical and physical testing.

Figure 4: **C**ubic molds for specimen preparation: (a) Front view of the mold with dimensions and (b) Molds.

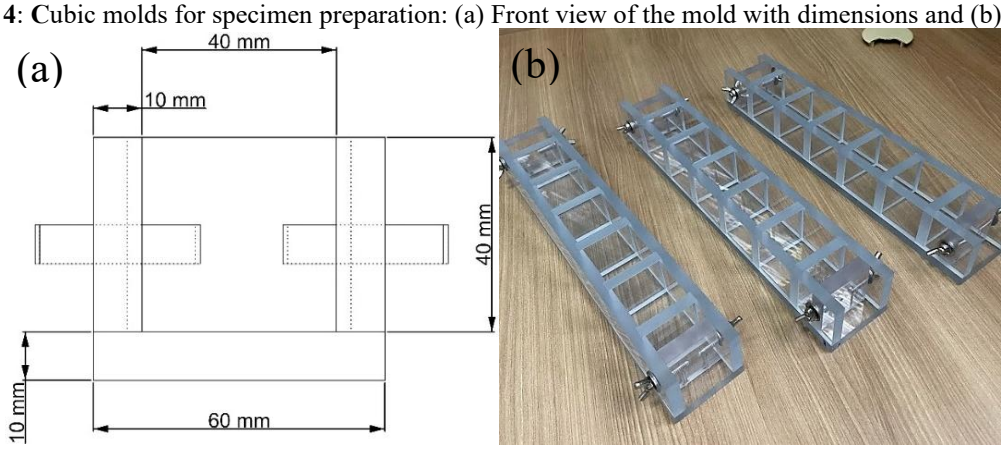

After molding, the specimens were subjected to three different curing regimes: (i) thermal curing, performed in a humidity chamber at a temperature of 60 °C and relative humidity of 90%, with the

samples sealed; (ii) curing at room temperature at 23 °C and 60% relative humidity; and (iii) curing at room temperature at 23 °C and 80% relative humidity, both conducted in a controlled climatic chamber until the testing age of 7 days. The comparison between the curing regimes was performed using compositions containing calcitic limestone, in order to isolate exclusively the effect of the curing type. In turn, the evaluation of the effect of the different fillers was conducted only under the room-temperature curing regime (23 °C) and 60% relative humidity.

2.3 TEST METHODS

The hydration reactions of the BMSC pastes were monitored using X-ray Diffraction (XRD) and Scanning Electron Microscopy (SEM). For the tests, the samples were ground in a Marconi MA590 mortar grinder and subsequently immersed in isopropyl alcohol to stop the hydration reactions. Only particles smaller than 75 μm (#325 mesh) were considered for the XRD tests. The tests were performed using a Horiba LA-960 X-ray diffractometer with CuKα radiation generated at a voltage of 40 kV and a current of 30 mA, over a scanning range of 5–65° (2θ) at a rate of 10°/min.

For the SEM test, fragments approximately 5 mm in length were embedded in epoxy resin, with a resin-to-catalyst ratio of 7:1, and after hardening, they were polished with silicon carbide metallographic abrasive papers. In order to perform quantitative analysis of the chemical composition of specific regions of the samples, they were examined by Energy-Dispersive X-ray Spectroscopy (EDS). The test was performed using a Hitachi TM3000 scanning electron microscope, while the EDS measurements were conducted with an Oxford Instruments SwiftED3000 spectrometer. The accelerating voltage used for the SEM analysis was 15 kV.

The physical properties were determined according to the ABNT NBR 9778 standard [43], evaluating the following properties: bulk density (BD), water absorption (WA), and apparent porosity (AP). The calculation is performed according to Eqs. (2), (3), and (4), respectively.

$$BD = \frac{M_S}{M_{SA} - M_I}\, x\, \rho \tag{2}$$

$$WA = \frac{M_{SA} - M_S}{M_S}\, x\, 100 \tag{3}$$

$$AP = \frac{M_{SA} - M_S}{M_{SA} - M_I} \tag{4}$$

Where M_{SA} is the mass of the water-saturated sample with a dry surface (g); M_S is the mass of the sample dried at 105 °C for 72 h (g); M_I is the mass of the sample immersed in water (g); ρ is the density of water (g/cm³).

The sample drying time of 72 h at 105 °C was determined in preliminary tests because shorter drying periods did not meet the requirements of the ABNT NBR 9778 standard, which stipulates that two successive weighings, at 24 h intervals, must not differ by more than 0.5% of the lower mass.

Compressive strength tests were conducted on cubic specimens (40 × 40 × 40) mm³, following the ASTM C109 standard [44]. The testing machine used was an EMIC CD 30000, equipped with a 5 kN load cell. The displacement rate was adjusted to 0.3 mm/min, and the final compressive strength for each mixture was calculated as the average obtained from six samples for each curing age (7 and 28 days).

3 RESULTS AND DISSCUSIONS

3.1 COMPRESSIVE STRENGTH OF BMSC PASTES

Figure 5 presents the compressive strength results of the BMSC and MOS samples after 7 days of curing. These samples were prepared with a MgO:$MgSO_4$ molar ratio of 10:1, with 20% by weight replacement of MgO with dolomitic limestone and oyster shell powder. In addition, citric acid was added at a

concentration of 0.5% by weight of MgO to the samples containing filler (BMSC CD+AC and BMSC OSP+AC).

As can be observed, the partial replacement of MgO with CD and OSP resulted in a decrease in the compressive strength of the reference MOS cement by approximately 30% and 25%, respectively, which can be attributed to the lower number of hydration phases formed due to the lower number of MgO nuclei. However, the addition of citric acid improved the compressive strength in both cases (CD and OSP). This improvement was more significant in the OSP+AC composition compared with the reference sample (MOS Ref), where the mechanical strength increased by approximately 78%. This increase in strength can be attributed to the formation of more stable hydration phases, such as phase 517, which has been reported as the phase with the best mechanical performance in BMSC [45], with its analysis performed in Section 3.3. In addition, the lower MgO content in the oyster shell powder may decrease the formation of $Mg(OH)_2$ and promote greater crystallization of phase 517.

Figure 5: Compressive strength of BMSC and MOS pastes cured for 7 days. *The same letters on different bars indicate that there is no statistically significant difference according to Tukey's test ($p < 0.05$, $n = 4$).

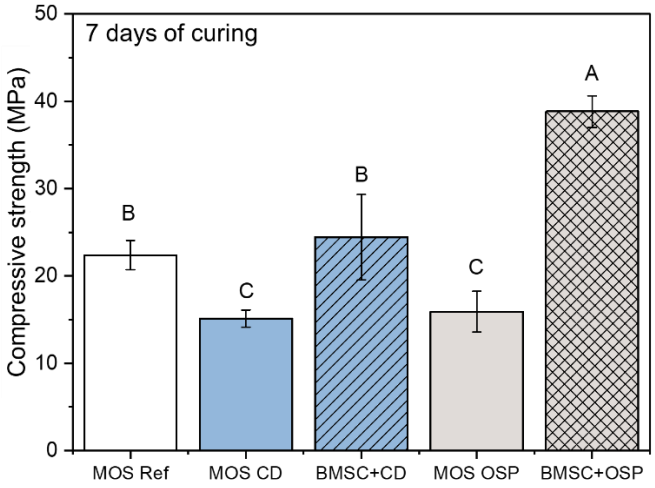

The comparison between BMSC produced with dolomitic limestone (CD) and calcitic limestone (CC) shows that the mineralogical composition of the filler directly influences the development of mechanical strength and the microstructural evolution of the cementitious system. Calcitic limestone, characterized by a higher $CaCO_3$ content and lower MgO content compared with CD, showed a tendency toward higher compressive strength values, a behavior also observed in the samples containing OSP. This result may be associated with the lower formation of brucite ($Mg(OH)_2$), a phase generally related to increased porosity and reduced matrix cohesion, as well as with the promotion of nucleation and growth of phase 517, recognized as the main product responsible for strength gain in BMSC. In addition, the lower magnesium content present in CC reduces competitive reactions during hydration, contributing to more efficient consumption of reactive MgO and to the formation of a more homogeneous and densified microstructure. This effect is potentially intensified by the smaller mean particle size of CC, which increases the available surface area and promotes a more pronounced filler effect, acting as a heterogeneous nucleation site for hydration products.

It is also observed that the curing regime plays a determining role in the evolution of mechanical strength. Curing in a climatic chamber under controlled conditions of approximately (24 ± 3) °C and (60 ± 5)% relative humidity provided the greatest strength gains, since this condition favors the stability of hydrated phases and reduces premature water evaporation, which is essential for the continuity of reactions in the $MgO–MgSO_4–H_2O$ system. In contrast, samples subjected to thermal curing exhibited the lowest compressive strength values, indicating that the increase in temperature accelerated the evaporation of free water and limited the progressive formation of more stable hydrated phases, particularly phase 517. The reduction in internal moisture during thermal curing tends to prematurely interrupt MgO hydration, resulting in a greater amount of unreacted MgO and a more porous and

heterogeneous microstructure. Additionally, air curing under lower relative humidity levels intensified surface carbonation processes and favored the early formation of less cohesive carbonated products, restricting mechanical gain at early ages. These results demonstrate that BMSC performance is strongly governed by water availability during curing, evidencing that the interaction between filler mineralogy, particle size, and curing conditions controls hydration kinetics and, consequently, the development of mechanical strength. Thus, the combination of calcitic filler and controlled curing under high humidity proved to be more efficient for optimizing the mechanical performance of BMSC.

Figure 6: Compressive strength of BMSC pastes with different types of limestone (A) under different curing regimes (B). *The same letters on different bars indicate that there is no statistically significant difference according to Tukey's test ($p < 0.05$, $n = 4$).

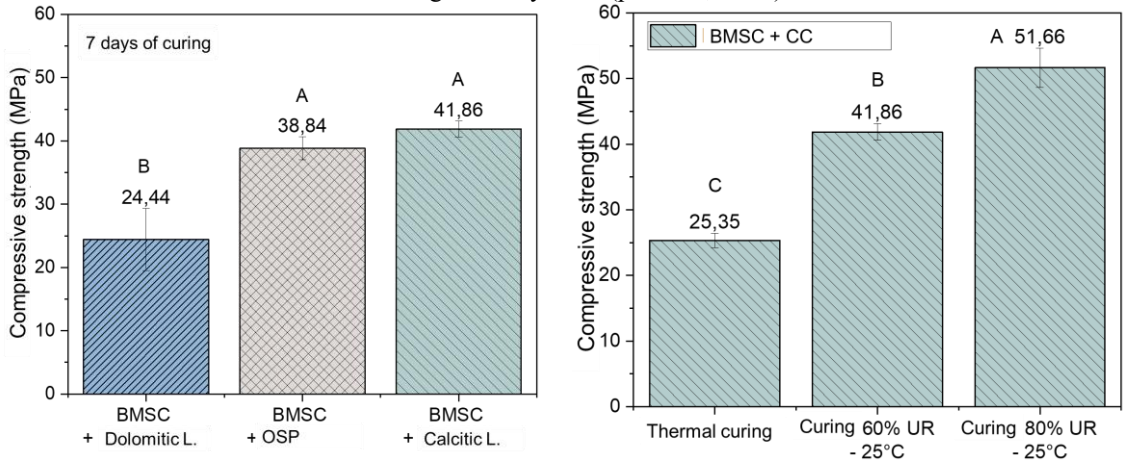

(A) (B)

3.2 PHYSICAL PROPERTIES

Figure 7 presents the results of water absorption (WA), apparent porosity (AP), and bulk density (BD) of the pastes after 7 days of controlled curing. The partial replacement of 20% of MgO with mineral fillers (CD and OSP) promoted a consistent increase in apparent porosity in all modified formulations compared with the reference MOS. As observed in Figure 7a, AP increased from approximately 33% in the MOS Ref formulation to values between 37 and 38% in the formulations containing fillers, corresponding to a relative increase of approximately 12–15%. This behavior is associated with the reduction in the content of reactive MgO available for the initial formation of hydration products, resulting in a greater volume of accessible voids in the cementitious matrix.

The increase in apparent porosity was accompanied by an increase in water absorption, which increased from approximately 23% in the reference formulation to values between 26 and 27% in the formulations containing fillers and citric acid. This result confirms the direct relationship between the increase in open pore volume and the greater absorption capacity of the matrix. However, unlike the behavior observed for porosity, bulk density showed a slight increase with the incorporation of fillers, varying from approximately 2.20 g/cm³ in MOS Ref to approximately 2.25–2.30 g/cm³ in the modified formulations. This behavior indicates that the replacement of MgO with fillers favored the packing of solid particles and the filling of intergranular voids [30], promoting a denser matrix, even with the increase in water-accessible porosity.

The incorporation of citric acid did not promote a significant reduction in apparent porosity, but contributed to stabilizing water absorption and improving the mechanical performance of the BMSC formulations. This effect may be related to the greater formation of phase 517, whose fiber-shaped morphology favors better interconnection between the hydration products and greater microstructural integrity of the matrix. Thus, the results suggest that the mechanical properties observed in Figures 5 and 6 do not depend exclusively on total porosity, but also on the microstructural organization of the matrix and the bonding efficiency between the hydrated phases. Even with the increase in AP, the

formulations containing fillers maintained compatible mechanical performance due to the combined effect of physical packing of the limestone particles and the formation of more stable hydration products.

Figure 7: Water absorption vs. apparent porosity (left) and bulk density (right) of BMSC and MOS cements after 7 days of controlled curing.

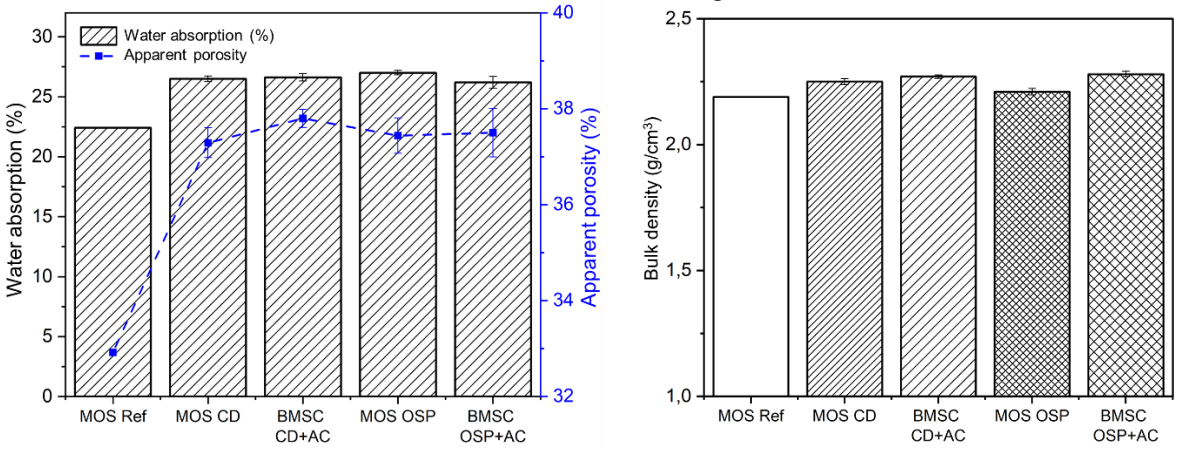

3.3 MINERALOGICAL ANALYSIS

The effect of the incorporation of CD and OSP and the addition of citric acid on the formation of hydration phases of the hardened cements after 7 days of curing is shown in Figure 8.

Figure 8: X-ray diffractograms of BMSC and MOS pastes cured for 7 days.

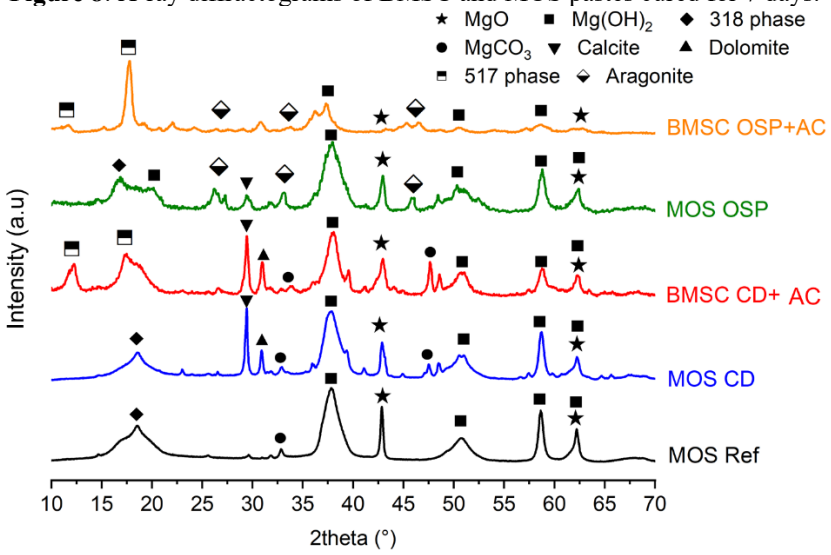

The results demonstrate that the main hydration products of the mixtures without the addition of citric acid consist of phase 318 ($3Mg(OH)_2 \cdot MgSO_4 \cdot 8H_2O$), $Mg(OH)_2$, and periclase (MgO), in addition to smaller amounts of phases with a lower degree of crystallinity, such as dolomite ($CaMg(CO_3)_2$), magnesite ($MgCO_3$), calcite ($CaCO_3$), and aragonite ($CaCO_3$). On the other hand, the addition of the chemical additive (AC) promoted the formation of phase 517, reported as the phase with the best mechanical performance in MOS cement [46]. Consequently, the OSP+AC and CD+AC samples obtained the best compressive strength results. In the microstructural analysis, the difference in the morphology of phases 318 and 517 can be observed, with phase 517 presenting long fiber-like forms similar to needles or whiskers, which increases mechanical strength due to the space-filling effect. Phase 517 was observed with greater intensity in the OSP+AC sample, resulting in a 78% increase in mechanical strength compared with the reference MOS cement. The presence of $MgCO_3$ in some compositions can be attributed to carbonation of the paste surface [23]. In addition, the replacement of MgO with CD and OSP reduced the amount of unhydrated MgO at 7 days and the formation of

$Mg(OH)_2$, and promoted the formation of new phases of dolomite, calcite, and aragonite. The lower formation of brucite at early curing ages resulted in lower mechanical strengths at 7 days for the samples without AC.

Figure 9 presents the X-ray diffractograms of BMSC pastes subjected to different curing regimes (thermal curing, 60% RH, and 80% RH), demonstrating the direct influence of curing conditions on the formation and stability of crystalline phases in the $MgO–MgSO_4–H_2O$ system. It can be observed that samples cured at 80% relative humidity exhibit greater intensity of the peaks attributed to phase 517, indicating a higher degree of hydration and formation of the main product responsible for mechanical strength gain, in agreement with the mechanical results obtained. Greater moisture availability favors the continuity of MgO hydration reactions and the stabilization of hydrated phases, reducing the relative presence of unreacted MgO.

Figure 9: X-ray diffractograms of BMSC + CD pastes under different curing regimes for 7 days.

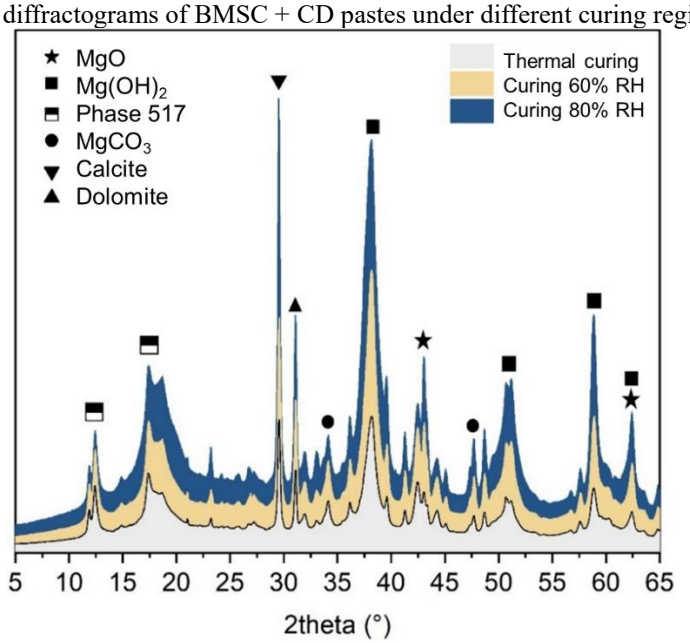

In contrast, thermal curing presents lower intensity of phase 517 and greater formation of $Mg(OH)_2$, suggesting incomplete hydration due to accelerated water evaporation, which limits crystal growth and results in a less dense microstructure. The samples cured at 60% RH exhibit intermediate behavior, with partial formation of phase 517 and a greater relative contribution of carbonated phases ($MgCO_3$), associated with surface carbonation favored by lower water availability. These results confirm that high relative humidity acts as a critical parameter for hydration kinetics and for the stabilization of phase 517, explaining the superior mechanical performance observed in samples cured at 80% RH.

3.4 MICROSTRUCTURAL ANALYSIS

Figure 10 shows SEM images of the MOS cement samples after 7 days of curing. The XRD and EDS results indicate that the lamellar crystalline phase is $Mg(OH)_2$, while phases 318 and 517 begin to form and grow at the solid-liquid interface of the $Mg(OH)_2$ crystals. The higher compressive strength results obtained for the BMSC OSP+AC and BMSC CD+AC matrices (Figure 5) are due to the needle-shaped crystals of phase 517, which increase the compactness of the MOS cement compared with the reference matrix, which presents greater formation of $Mg(OH)_2$ flakes and lower porosity, as observed in Figures (B), (H), and (J). On the other hand, the filler particles did not show the formation of crystallization phases on their surface, and greater porosity can be observed in the microstructures shown in Figures (C) and (G) in the case of the samples with CD, which was also confirmed by the apparent porosity tests. The morphology and higher pore content in the samples with CD and OSP containing citric acid can relieve the internal stresses produced by the expansion of MgO hydration during air curing and improve the long-term mechanical strengths [47].

Figure 10: Fractured surface morphology of BMSC and MOS samples after 7 days of curing.

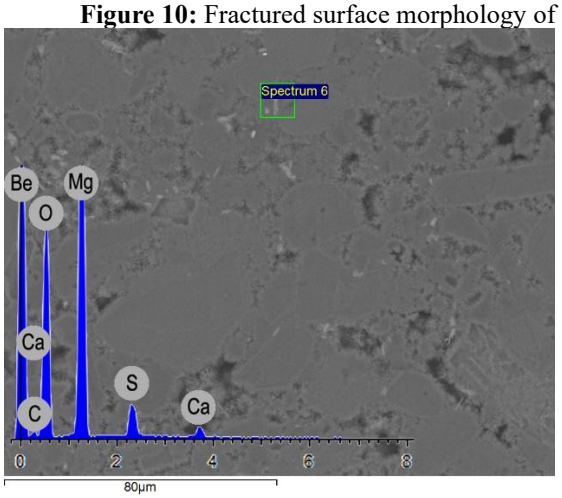

(A) MOS Ref

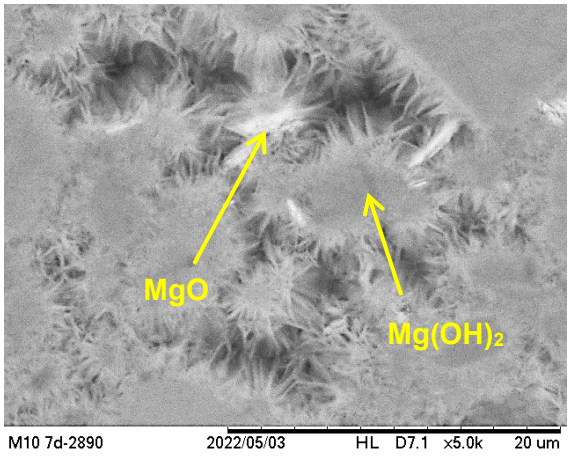

(B) MOS Ref x5.0k

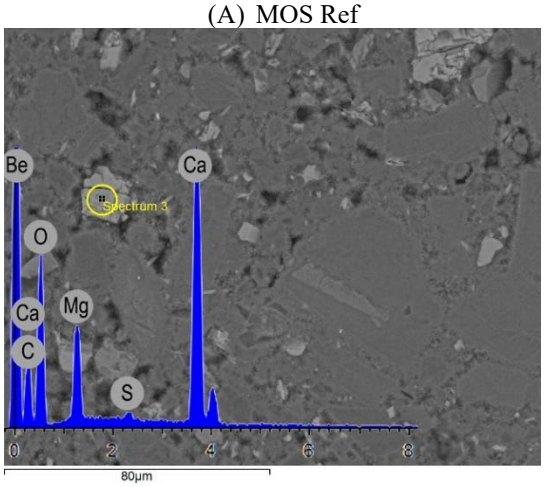

(C) MOS CD

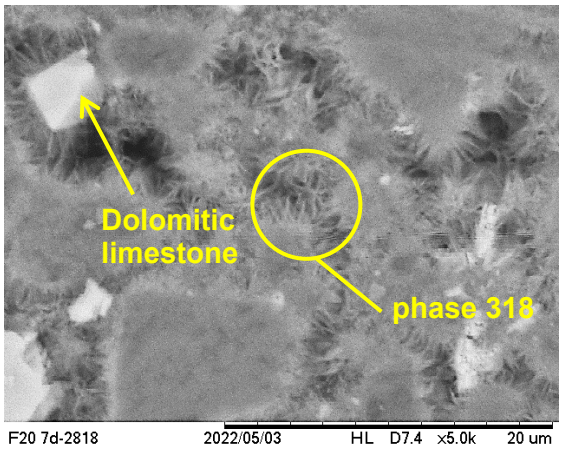

(D) MOS CD x5.0k

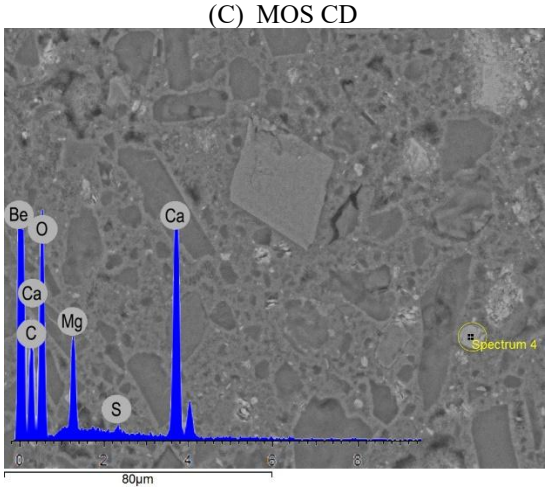

(E) MOS OSP

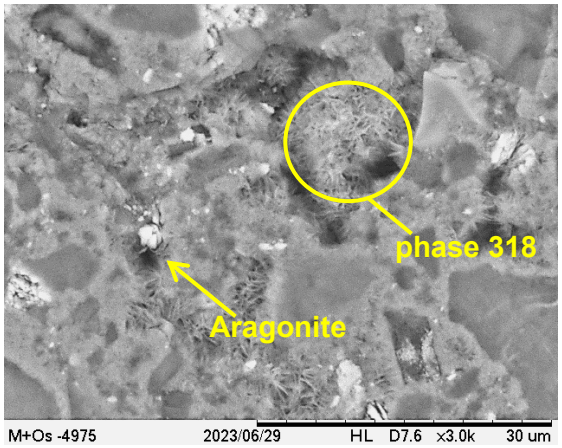

(F) MOS OSP x5.0k

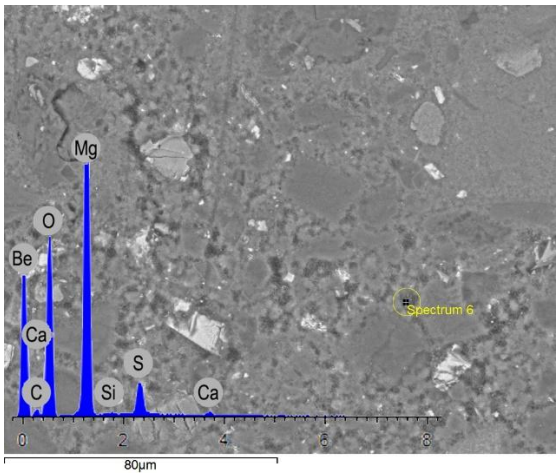

(G) BMSC CD+AC

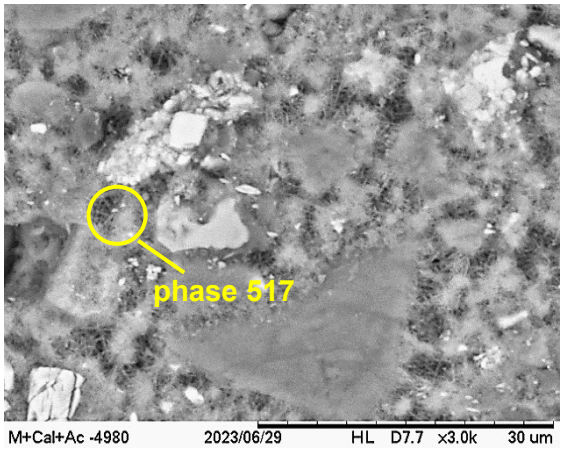

(H) BMSC CD+AC x5.0k

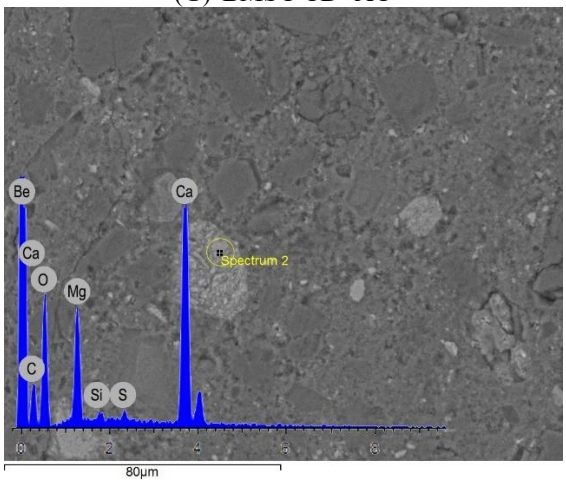

(I) BMSC OSP+AC

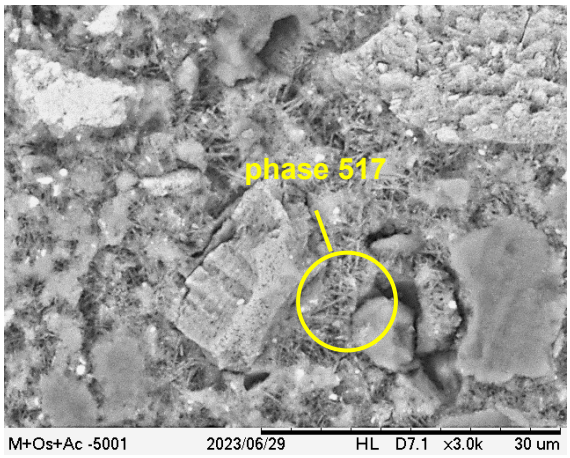

(J) BMSC OSP+AC x5.0k

4 CONCLUSIONS

In this study, magnesium oxysulfate (MOS) cements, also referred to as basic magnesium sulfate cement (BMSC), containing different mineral limestone additions as partial replacements for MgO were developed, with the objective of evaluating the influence of filler mineralogy and curing conditions on the mechanical and physical properties and on the formation of hydration phases. The associated mechanisms were investigated through the analysis of compressive strength, water absorption, apparent porosity, bulk density, X-ray diffraction (XRD), and scanning electron microscopy (SEM). Additionally, different curing regimes were evaluated in order to understand their influence on the microstructural evolution and the development of the properties of the MOS system. The study highlights the following conclusions:

- The lower content of the hydration product, phase 318, and the lower formation of brucite at early curing times decrease the mechanical strength of MOS cement prepared without chemical additives.
- The formation of hydration phase 517, due to the incorporation of citric acid (AC), demonstrated an increase in the mechanical strength of the cement. This phenomenon can be attributed to the fiber-shaped morphology of the phase, resulting in a lower surface area, in addition to the filler effect of the limestone particles.
- The increase in porosity in the microstructure of BMSC and MOS pastes, due to the replacement of MgO by the filler, can relieve the internal stresses produced by the expansion of MgO hydration during air curing and prevent the loss of mechanical strength.
- The curing conditions directly influenced the formation of the hydrated phases of BMSC cement, with curing at room temperature with 80% relative humidity promoting the highest intensity of phase 517 and, consequently, the highest mechanical strength values.

ACKNOWLEDGEMENTS

The authors would like to thank the funding agency Coordination for the Improvement of Higher Education Personnel (CAPES), funding code 001, the São Paulo Research Foundation (FAPESP) – Processes: 23/04412-3 and 24/02445-4, the National Council for Scientific and Technological Development (CNPq) – Processes: 422701/2021-1, as well as the INCT Institute of Innovation in Eco-efficient Cementitious Materials for Construction Decarbonization – IMCEDEC.

REFERENCES

[1] M. A. Shand, "Magnesium oxysulfate cement," in *Magnesia Cements*, Elsevier, 2020, pp. 75–83. doi: 10.1016/B978-0-12-391925-0.00010-8.

[2] S. A. Walling and J. L. Provis, "Magnesia-based cements: A journey of 150 years, and cements for the future?," *Chem. Rev.*, vol. 116, no. 7, pp. 4170–4204, Apr. 2016. doi: 10.1021/acs.chemrev.5b00463.

[3] M. Ba, T. Xue, Z. He, H. Wang, and J. Liu, "Carbonation of magnesium oxysulfate cement and its influence on mechanical performance," *Constr. Build. Mater.*, vol. 223, pp. 1030–1037, Oct. 2019. doi: 10.1016/j.conbuildmat.2019.07.341.

[4] G. C. E. Marmorato and C. Gladis, "Magnesium oxysulfate fibercement," *Key Eng. Mater.*, vol. 600, pp. 308–318, 2014. doi: 10.4028/www.scientific.net/KEM.600.308.

[5] Y. Tan, C. Wu, H. Yu, Y. Li, and J. Wen, "Review of reactive magnesia-based cementitious materials: Current developments and potential applicability," *J. Build. Eng.*, vol. 40, p. 102342, Aug. 2021. doi: 10.1016/j.jobe.2021.102342.

[6] W. Yu, H. Yu, H. Ma, T. Shi, J. Wen, H. Ma, L. Li, and X. Chen, "Basic magnesium sulfate cement products exposed to air at various exposure ages: Phase composition, microstructure, and mechanical characteristics," *J. Build. Eng.*, vol. 79, p. 107799, Dec. 2023. doi: 10.1016/j.jobe.2023.107799.

[7] Y. Tan, H. Yu, D. Yang, and T. Feng, "Basic magnesium sulfate cement: Autogenous shrinkage evolution and mechanism under various chemical admixtures," *Cem. Concr. Compos.*, vol. 128, p. 104412, Apr. 2022. doi: 10.1016/j.cemconcomp.2022.104412.

[8] L. Wang, S. S. Chen, D. C. W. Tsang, C. S. Poon, and K. Shih, "Recycling contaminated wood into eco-friendly particleboard using green cement and carbon dioxide curing," *J. Clean. Prod.*, vol. 137, pp. 861–870, Nov. 2016. doi: 10.1016/j.jclepro.2016.07.180.

[9] L. Qin, X. Gao, and T. Chen, "Recycling of raw rice husk to manufacture magnesium oxysulfate cement based lightweight building materials," *J. Clean. Prod.*, vol. 191, pp. 220–232, Aug. 2018. doi: 10.1016/j.jclepro.2018.04.238.

[10] N. José, H. Ahmed, B. Miguel, E. Luís, and J. de Brito, "Magnesia (MgO) production and characterization, and its influence on the performance of cementitious materials: A review," *Materials*, vol. 13, no. 21, p. 4752, Oct. 2020. doi: 10.3390/ma13214752.

[11] Q. Sun, M. Ba, D. Zhang, S. Zhou, N. Zhang, and F. Wang, "Effects of citrate acid, solidum silicate and their compound on the properties of magnesium oxysulfate cement under carbonation condition," *Constr. Build. Mater.*, vol. 330, p. 127136, May 2022. doi: 10.1016/j.conbuildmat.2022.127136.

[12] C. K. Chau, J. Chan, and Z. Li, "Influences of fly ash on magnesium oxychloride mortar," *Cem. Concr. Compos.*, vol. 31, no. 4, pp. 250–254, Apr. 2009. doi: 10.1016/j.cemconcomp.2009.02.011.

[13] C. M. Gomes and A. D. S. de Oliveira, "Chemical phases and microstructural analysis of pastes based on magnesia cement," *Constr. Build. Mater.*, vol. 188, pp. 615–620, Nov. 2018. doi: 10.1016/j.conbuildmat.2018.08.083.

[14] M. Liska, A. Al-Tabbaa, K. Carter, and J. Fifield, "Scaled-up commercial production of reactive magnesium cement pressed masonry units. Part I: Production," *Proc. Inst. Civ. Eng. Constr. Mater.*, vol. 165, no. 4, pp. 211–223, Aug. 2012. doi: 10.1680/coma.10.00032.

[15] U.S. Geological Survey, "Mineral commodity summaries 2022," U.S. Geological Survey, Reston, VA, USA, Tech. Rep., 2022.

[16] T. Demediuk and W. F. Cole, "A study of magnesium oxysulphates," *Aust. J. Chem.*, vol. 10, no. 3, pp. 287–294, 1957. doi: 10.1071/CH9570287.

[17] M. Ba, Q. Gao, Y. Ma, J. Zhu, and Y. Du, "Improved hydration and properties of magnesium oxysulfate (MOS) cement using sodium silicate as an additive," *Constr. Build. Mater.*, vol. 267, p. 120988, Jan. 2021. doi: 10.1016/j.conbuildmat.2020.120988.

[18] C. M. Gomes, N. Cheung, G. M. Gomes, A. K. Sousa, and A. P. Peruzzi, "Improvement of water resistance in magnesia cements with renewable source silica," *Constr. Build. Mater.*, vol. 272, p. 121650, Feb. 2021. doi: 10.1016/j.conbuildmat.2020.121650.

[19] J. C. A. Molano, A. G. S. Azevedo, T. O. G. Freitas, G. C. Da Silva, and H. Savastano, "Effects of dolomitic limestone on the properties of magnesium oxysulfate cement," *Materials*, vol. 17, no. 18, p. 4580, Sep. 2024. doi: 10.3390/ma17184580.

[20] D. H. Deng, "The theories and the practical techniques improve the properties of MgO-based basic cement," Ph.D. dissertation, Central South University, Changsha, China, 2005.

[21] T. Runčevski, C. Wu, H. Yu, B. Yang, and R. E. Dinnebier, "Structural characterization of a new magnesium oxysulfate hydrate cement phase and its surface reactions with atmospheric carbon dioxide," *J. Am. Ceram. Soc.*, vol. 96, no. 11, pp. 3609–3616, Nov. 2013. doi: 10.1111/jace.12556.

[22] W. Chengyou, "Fundamental theory and civil engineering application of basic magnesium sulfate cement," Ph.D. dissertation, Univ. of Chinese Academy of Sciences, Beijing, China, 2014, pp. 147–151.

[23] S. Tang, J. Yuan, R. Cai, C. Wei, J. Chen, and E. Chen, "In situ monitoring of hydration of magnesium oxysulfate cement paste: Effect of MgO/MgSO4 ratio," *Constr. Build. Mater.*, vol. 251, p. 119003, Aug. 2020. doi: 10.1016/j.conbuildmat.2020.119003.

[24] S. Tang, C. Wei, R. Cai, J. Huang, E. Chen, and J. Yuan, "In situ monitoring of pore structure of magnesium oxysulfate cement paste: Effect of MgSO4/H2O ratio," *J. Ind. Eng. Chem.*, vol. 83, pp. 387–400, Mar. 2020. doi: 10.1016/j.jiec.2019.12.012.

[25] V. M. John, B. L. Damineli, M. Quattrone, and R. G. Pileggi, "Fillers in cementitious materials — Experience, recent advances and future potential," *Cem. Concr. Res.*, vol. 114, pp. 65–78, Dec. 2018. doi: 10.1016/j.cemconres.2017.09.013.

[26] D. K. Panesar and R. Zhang, "Performance comparison of cement replacing materials in concrete: Limestone fillers and supplementary cementing materials – A review," *Constr. Build. Mater.*, vol. 251, p. 118866, Aug. 2020. doi: 10.1016/j.conbuildmat.2020.118866.
[27] B. L. Damineli, R. G. Pileggi, B. Lagerblad, and V. M. John, "Effects of filler mineralogy on the compressive strength of cementitious mortars," *Constr. Build. Mater.*, vol. 299, p. 124363, Sep. 2021. doi: 10.1016/j.conbuildmat.2021.124363.
[28] V. T. Luong, R. Amal, J. A. Scott, S. Ehrenberger, and T. Tran, "A comparison of carbon footprints of magnesium oxide and magnesium hydroxide produced from conventional processes," *J. Clean. Prod.*, vol. 202, pp. 1035–1044, Nov. 2018. doi: 10.1016/j.jclepro.2018.08.225.
[29] *Fibre-cement flat sheets — Product specification and test methods*, ISO Standard 8336, 2017.
[30] S. Ruan and C. Unluer, "Influence of supplementary cementitious materials on the performance and environmental impacts of reactive magnesia cement concrete," *J. Clean. Prod.*, vol. 159, pp. 62–73, Aug. 2017. doi: 10.1016/j.jclepro.2017.05.044.
[31] Q. Li, A. Su, and X. Gao, "Preparation of durable magnesium oxysulfate cement with the incorporation of mineral admixtures and sequestration of carbon dioxide," *Sci. Total Environ.*, vol. 809, p. 152127, Feb. 2022. doi: 10.1016/j.scitotenv.2021.152127.
[32] Z. Li, Y. Hua, Z. Chang, Y. Yue, J. Qin, and J. Qian, "Hydration, carbonation and strength development of reactive MgO cement blended with lime (CaO) under different curing conditions," *J. Build. Eng.*, vol. 76, p. 107082, Oct. 2023. doi: 10.1016/j.jobe.2023.107082.
[33] C. M. Gomes and A. K. D. S. de Oliveira, "Effects of filler carbonates on magnesium-oxide based pastes," *Constr. Build. Mater.*, vol. 262, p. 119913, Nov. 2020. doi: 10.1016/j.conbuildmat.2020.119913.
[34] I. dos S. Pereira, A. L. Bamberg, R. O. de Sousa, A. B. Monteiro, R. Martinazzo, C. A. P. Silveira, and A. de O. Silveira, "Agricultural use and pH correction of anaerobic sewage sludge with acid pH," *J. Environ. Manage.*, vol. 275, p. 111203, Dec. 2020. doi: 10.1016/j.jenvman.2020.111203.
[35] D. Palma, L. T. Fuess, A. N. de Lima-Model, K. Z. da Conceição, M. P. Cereda, M. H. F. Tavares, and S. D. Gomes, "Using dolomitic limestone to replace conventional alkalinization in the biodigestion of rapid acidification cassava processing wastewater," *J. Clean. Prod.*, vol. 172, pp. 2942–2953, Jan. 2018. doi: 10.1016/j.jclepro.2017.11.118.
[36] *Caustic burned magnesia for magnesium oxychloride cement products*, WB/T Standard 1019-2002, State Commission for Economic and Trade, Beijing, China, 2002.
[37] H. F. Dong, L. M. Yu, and J. M. Zhang, "Study on experimental conditions of hydration methods of determining active magnesium oxide content," *J. Salt Lake Res.*, vol. 18, pp. 38–41, 2010.
[38] K. Gu, B. Chen, H. Yu, N. Zhang, W. Bi, and Y. Guan, "Characterization of magnesium-calcium oxysulfate cement prepared by replacing MgSO4 in magnesium oxysulfate cement with untreated desulfurization gypsum," *Cem. Concr. Compos.*, vol. 121, p. 104091, Aug. 2021. doi: 10.1016/j.cemconcomp.2021.104091.
[39] R. Wang, L. Qin, and X. Gao, "Mechanical strength and water resistance of magnesium oxysulfate cement based lightweight materials," *Cem. Concr. Compos.*, vol. 109, p. 103554, May 2020. doi: 10.1016/j.cemconcomp.2020.103554.
[40] Y. Hao, C. Li, and F. Zhao, "Study on water resistance modification of magnesium oxysulfate cement," *IOP Conf. Ser.: Mater. Sci. Eng.*, vol. 493, p. 012079, Mar. 2019. doi: 10.1088/1757-899X/493/1/012079.
[41] A. Azevedo, J. Adrada, I. Parente, T. Freitas, A. C. Azevedo, M. P. Faria, and H. Savastano, "Physical-mechanical properties of effect of rehydration on the physical-mechanical properties of CO2-cured magnesium-based fiber cement boards," *Eng. Civil (Preprint)*, 2023. doi: 10.20944/preprints202311.0038.v1.
[42] A. G. S. Azevedo, T. O. G. Freitas, J. C. A. Molano, H. R. Trevisan, I. M. S. Parente, P. Faria, A. Camões, and H. Savastano, "Assessment of the physical-mechanical performance of magnesium oxide-based fiber cement submitted to accelerated carbonation," *Cerâmica*, vol. 69, pp. 312–317, 2023. doi: 10.1590/0366-69132024703923500.
[43] *Argamassa e concreto endurecidos - Determinação da absorção de água, índice de vazios e massa específica*, ABNT NBR Standard 9778, 2005.
[44] *Standard Test Method for Compressive Strength of Hydraulic Cement Mortars (Using 2-in. or [50-mm] Cube Specimens)*, ASTM Standard C109/C109M, 2020.
[45] Y. Tan, H. Yu, S. Sun, C. Wu, and H. Ding, "Properties and microstructure of basic magnesium sulfate cement: Influence of silica fume," *Constr. Build. Mater.*, vol. 266, p. 121076, Jan. 2021. doi: 10.1016/j.conbuildmat.2020.121076.
[46] N. Wang, H. Yu, W. Bi, Y. Tan, N. Zhang, C. Wu, H. Ma, and S. Hua, "Effects of sodium citrate and citric acid on the properties of magnesium oxysulfate cement," *Constr. Build. Mater.*, vol. 169, pp. 697–704, Apr. 2018. doi: 10.1016/j.conbuildmat.2018.02.208.
[47] R. Wang, L. Qin, and X. Gao, "Mechanical strength and water resistance of magnesium oxysulfate cement based lightweight materials," *Cem. Concr. Compos.*, vol. 109, p. 103554, May 2020. doi: 10.1016/j.cemconcomp.2020.103554.

Author Contributions: J.C.A.M.: Conceptualization, Data Curation, Formal Analysis, Writing – original draft; Writing – review & editing. **H.S.J.:** Methodology, Writing – review & editing, Supervision. **D.S.L.**: Methodology, Data Curation, Formal Analysis, Writing – review & editing. **K.P.C.:** Data Curation, Formal Analysis, Writing – review & editing. **A.G.A.:** Formal Analysis, Writing – review & editing, Supervision**.**